REPORT DOCUMENTATION PAGE

Form Approved
OMB No. 0704-0188

1. REPORT DATE *(DD-MM-YYYY)*
21-11-2005

REPRINT

4. TITLE AND SUBTITLE
QUANTUM LATTICE-GAS MODEL FOR THE DIFFUSION EQUATION

5a. CONTRACT NUMBER

5b. GRANT NUMBER

5c. PROGRAM ELEMENT NUMBER
61102F

6. AUTHOR(S)
J. Yepez

5d. PROJECT NUMBER
2304

5e. TASK NUMBER
0T

5f. WORK UNIT NUMBER
B1

7. PERFORMING ORGANIZATION NAME(S) AND ADDRESS(ES)
Air Force Research Laboratory/VSBYA
29 Randolph Road
Hanscom AFB MA 01731-3010

8. PERFORMING ORGANIZATION REPORT NUMBER
AFRL-VS-HA-TR-2005-1167

9. SPONSORING / MONITORING AGENCY NAME(S) AND ADDRESS(ES)

10. SPONSOR/MONITOR'S ACRONYM(S)

11. SPONSOR/MONITOR'S REPORT NUMBER(S)

12. DISTRIBUTION / AVAILABILITY STATEMENT
Approved for Public Release; Distribution Unlimited.

13. SUPPLEMENTARY NOTES
REPRINTED FROM: INTERNATIONAL JOURNAL OF MODERN PHYSICS C, Vol 12, No. 9, (2001) 1285-1303

14. ABSTRACT

Presented is a factorized quantum lattice-gas algorithm to model the diffusion equation. It is a minimal model with two qubits per node of a one-dimensional lattice and it is suitable for implementation on a large array of small quantum computers interconnected by nearest-neighbor classical communication channels. The quantum lattice-gas system is described at the mesoscopic scale by a lattice-Boltzmann equation whose collision term is unconditionally stable and obeys the principle of detailed balance. An analytical treatment of the model is given to predict a macroscopic effective field theory. The numerical simulations are in excellent agreement with the analytical results. In particular, numerical simulations confirm the value of the analytically calculated diffusion constant. The algorithm is time-explicit with numerical convergence that is first-order accurate in time and second-order accurate in space.

15. SUBJECT TERM:
Quantum computation Quantum lattice gas Diffusion equation
Type-II quantum computer

16. SECURITY CLASSIFICATION OF:			17. LIMITATION OF ABSTRACT	18. NUMBER OF PAGES	19a. NAME OF RESPONSIBLE PERSON
a. REPORT		c. THIS PAGE			Jeffrey Yepez
UNCLAS	UNCLAS	UNCLAS	SAR		19b. TELEPHONE NUMBER *(include area code)* 781-377-5957

International Journal of Modern Physics C, Vol. 12, No. 9 (2001) 1285-1303

World Scientific Publishing Company

Quantum Lattice-Gas Model for the Diffusion Equation

Jeffrey Yepez*

Air Force Research Laboratory, Hanscom Field, Massachusetts 01731

Jeffrey.Yepez@hanscom.af.mil

http://qubit.plh.af.mil/

August 16, 2000

Received 20 December 2000

Revised 9 April 2001

Abstract

Presented is a factorized quantum lattice-gas algorithm to model the diffusion equation. It is a minimal model with two qubits per node of a one-dimensional lattice and it is suitable for implementation on a large array of small quantum computers interconnected by nearest-neighbor classical communication channels. The quantum lattice-gas system is described at the mesoscopic scale by a lattice-Boltzmann equation whose collision term is unconditionally stable and obeys the principle of detailed balance. An analytical treatment of the model is given to predict a macroscopic effective field theory. The numerical simulations are in excellent agreement with the analytical results. In particular, numerical simulations confirm the value of the analytically calculated diffusion constant. The algorithm is time-explicit with numerical convergence that is first-order accurate in time and second-order accurate in space.

Keywords: Quantum computation; quantum lattice gas; diffusion equation; type-II quantum computer.

1 Introduction

For the purpose of testing quantum lattice-gas dynamics on a *type II quantum computer* (a massively parallel array of small quantum computers) [1], it is prudent to use the simplest of models so that results from prototype experimental

*This work was supported by the Air Force Office of Scientific Research Directorate of Mathematics and Space Sciences task No. 2304TD.

implementations can most readily and easily be compared to results obtained by numerical simulations on conventional computers[1]. Another reason to test simple quantum lattice-gas models is that the prediction of solutions obtained with the quantum algorithm can be compared against exact solutions obtained by analytical means. The simplest lattice-gas models are one-dimensional [2, 3] and have only a single conserved quantity, the particle number. The macroscopic field, well defined in the continuum limit and which corresponds to microscopic particle conservation, is the *mass-density* field. The simplest particle conserving dynamics is diffusion. Therefore, presented in this paper is a quantum lattice-gas model that can be used to simulate the behavior of a macroscopic mass-density field governed by a parabolic diffusion equation in the long-wavelength limit.

The quantum computer is comprised of a large even number of qubits. Each qubit is a two-energy level quantum system [4, 5]. The high-energy quantum state is called *one* and the low-energy quantum state is called *zero*. The quantum algorithm presented in this paper requires the measurement of these binary states after the application of every two-qubit quantum gate operation. Therefore, quantum phase coherence need only persist between only two qubits for the short duration of time needed to complete a quantum gate operation. Furthermore, the probability of occupancy of the binary quantum states of each qubit must be accurately measured.

The algorithm presented in this paper is part quantum mechanical and part classical. The quantum part of the algorithm requires quantum state preparation, application of a two-qubit quantum gate [6, 7, 8], and measurement of each of the probability of occupancies of the one and zero states of both qubits involved in each quantum gate operation. Consequently, the state preparation, quantum gate operation, and measurement process must be either repeated in time over and over again on a pairs of qubits, or a large ensemble of qubit pairs must be simultaneously initialized, quantum mechanically operated upon, and measured in order to obtain a good estimate of the probability of occupancy of their one and zero states. The classical part of the algorithm involves transferring information between qubit pairs. This is done by preparing the state of some qubit in the quantum computer to be equal to the state of some other qubit that was previously measured in the quantum computer. Classical information (the probability of occupancy known to some level of precision) is therefore transferred between qubit pairs.

The algorithm can give rise to nontrivial macroscopic scale behavior of the quantum computer because the set of qubit pairs that the quantum gates act upon is different than the set of qubit pairs between which classical state information is exchanged. The quantum gate operations and the exchange of classical state information is set up to allow for the computation of the time

[1] A type-II quantum computer prototype is presently under joint development by the Air Force Research Laboratory and the department of Nuclear Engineering at MIT using a spatial nuclear magnetic resonance spectroscopic technique. The algorithm presented in this paper, in particular the unitary quantum gate (8), serves as a baseline numerical test case for the quantum computing experiment. All the simulation results presented in this paper where carried on a conventional desktop computer.

evolution of a factorized quantum lattice-gas system [9, 10]. The adjective *factorized* is used here to indicate that the lattice-gas system undergoes continual and repeated measurement throughout the system. Looked upon as a many-body particle system, the kinetic behavior the factorized quantum lattice gas at the mesoscopic scale[2] is described by a Boltzmann equation, whose collision term is expressible in factorizable form typical of a mean-field approximation to the collision process.

This paper is divided into four parts. In the first part, §2, we describe the basic formulation of the quantum lattice-gas algorithm. The collision operator for the model is a two-qubit quantum gate. In the second part, §3, all the steps needed to implement the algorithm are explicitly presented. The collision operator is chosen to be a symmetric matrix. The emergent behavior of the mass-density field at the macroscopic scale is not biased and, therefore, causes the particles to drift equally either to the left or the right. As in any lattice-gas algorithm, the dynamics are reduced to mutually exclusive collision and streaming events. That is, in a completely artificial and discretized way, the particles at each site first collide and then they hop to neighboring sites of the lattice. There are two speed-one particles per site, one particle moves to the right and the other to the left. The collision operator is homogeneously and simultaneously applied across the lattice and then the particles hops one lattice unit to the right and left respectively. Therefore, each and every time step involves a single application of the collision operator and streaming operator. In the third part, §4, we analyze the behavior of the model using an exact lattice Boltzmann equation description that holds at the mesoscopic scale. We show why the macroscopic scale behavior of the factorized quantum lattice-gas system is described by a diffusion equation with a constant transport coefficient of one half for our particular choice of the collision operator. In the forth part, §5, we carry out numerical simulations and compare the computed results with the analytical results obtained in §4. Numerical estimates of dispersion and damping of the mass-density field are in excellent agreement with exact analytical predictions and this conclusively indicates the macroscopic scale behavior of the quantum lattice gas is described by a parabolic diffusion equation. The L_2 norm of the error is also measured for multiple simulations of varying grid resolutions and we find that the quantum algorithm has numerical convergence with first-order accuracy in time and second-order order accuracy in space.

2 Model Formulation

Consider the quantum computer with L number of nodes depicted in Figure 1. There are two qubits per node that may remain phase coherent for a short

[2] The mesoscopic scale is a regime between the microscopic and macroscopic scales where the probability of finding a particle in a local quantum state is well-defined. Although the occupancy probabilities are continuous quantities at the mesoscopic scale, the mesoscopic particle dynamics are still spatially and temporally discrete. Continuous field quantities, such as the mass-density field, are well defined only when the cell size of the mesoscopic lattice approaches zero, which is referred to as the *continuum limit*.

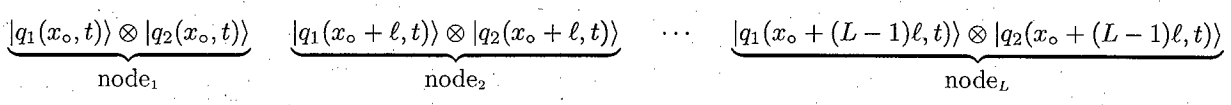

Figure 1: Depiction of a type II quantum computer with L nodes and 2 qubits per node. The array is one dimensional with periodic boundary conditions. The coordinate $x_\circ$ refers to the location of the first node. The symbol $\otimes$ represents the tensor (or outer) product operation.

duration in time. Initially, the state of each qubit

$$|q_a(x,t)\rangle = \alpha_a|0\rangle + \beta_a|1\rangle \tag{1}$$

is independently set (with the constraint $|\alpha_a|^2 + |\beta_a|^2 = 1$) so that the *on-site ket*, $|\psi(x,t)\rangle$, is a tensor product over the qubit residing at site x

$$|\psi(x,t)\rangle = |q_1(x,t)\rangle \otimes |q_2(x,t)\rangle, \tag{2}$$

for all x. Because there are two qubits per site, each on-site ket resides in a four dimensional Hilbert space. We use the following basis states

$$|00\rangle = \begin{pmatrix}0\\0\\0\\1\end{pmatrix} \quad |01\rangle = \begin{pmatrix}0\\0\\1\\0\end{pmatrix} \quad |10\rangle = \begin{pmatrix}0\\1\\0\\0\end{pmatrix} \quad |11\rangle = \begin{pmatrix}1\\0\\0\\0\end{pmatrix}. \tag{3}$$

In this basis, the number operators for the occupancy of qubits $|q_1\rangle$ and $|q_2\rangle$ are represented by the following matrices

$$\hat{n}_1 = \begin{pmatrix}1&0&0&0\\0&1&0&0\\0&0&0&0\\0&0&0&0\end{pmatrix} \quad \hat{n}_2 = \begin{pmatrix}1&0&0&0\\0&0&0&0\\0&0&1&0\\0&0&0&0\end{pmatrix}. \tag{4}$$

The *occupancy probability* of the a^{th} qubit at site x at time t is defined as follows

$$f_a(x,t) \equiv \langle\psi(x,t)|\hat{n}_a|\psi(x,t)\rangle, \tag{5}$$

for $a = 1, 2$. We define the "*mass density*" field as the sum of the occupancy probabilities[3]

$$\rho(x,t) \equiv f_1(x,t) + f_2(x,t). \tag{6}$$

In the continuum limit, where the lattice resolution becomes infinite, the mass density field is considered to be a continuous and differentiable field. Given an appropriate sequence of quantum gate operations applied to the quantum

[3] Here we have taken the mass of a particle to be unity, $m = 1$.

computer array depicted in Figure 1, the ρ field will evolve in time in a diffusive fashion. The dynamics is governed, in the long-wavelength limit, by the following parabolic partial differential equation of motion of the form

$$\frac{\partial \rho}{\partial t} = D \frac{\partial^2 \rho}{\partial x^2}. \tag{7}$$

The value of the diffusion constant, D, is determined by the choice of the quantum gate used to compute *outgoing configurations* and is also determined by the discrete particle movement on the one dimensional lattice used in this model.

Let us consider a particle-conserving dynamics. That is, we will choose to use a two-qubit quantum gate of the form

$$\hat{U} = \begin{pmatrix} 1 & 0 & 0 & 0 \\ 0 & e^{i\phi}e^{i\xi}\cos\theta & e^{i\phi}e^{i\zeta}\sin\theta & 0 \\ 0 & -e^{i\phi}e^{-i\zeta}\sin\theta & e^{i\phi}e^{-i\xi}\cos\theta & 0 \\ 0 & 0 & 0 & 1 \end{pmatrix}, \tag{8}$$

with a 2×2 unitary block which only mixes the states $|01\rangle$ and $|10\rangle$ and thereby conserves the particle number. This gate $\hat{U}$ is called the *collision operator*. So the outgoing configuration, encoded by the ket $|\psi'\rangle$, is computed independently on a site-by-site basis as follows

$$|\psi'(x,t)\rangle = \hat{U}|\psi(x,t)\rangle. \tag{9}$$

That is, the collisional operator is applied homogeneously across all lattice nodes. In general, $\hat{U}$ will cause quantum superposition and entanglement within each on-site manifold. The quantum superposition will persist for a length of time, here denoted by τ, corresponding to the spin-spin decoherence time of the quantum mechanically coupled qubits or until a measurement of the quantum state is performed.

3 Factorized Quantum Lattice-Gas Algorithm

The factorized quantum lattice-gas algorithm for the one-dimensional diffusion equation can be implemented in the following three steps. We assume the initial state of the quantum computer is set as specified in Figure 1, where $|q_a(x,t)\rangle = \sqrt{f_a(x,t)}|1\rangle + \sqrt{1-f_a(x,t)}|0\rangle$.

STEP 1: Apply the collision operator simultaneously to all sites

$$|\psi'(x,t)\rangle = \hat{U}|\psi(x,t)\rangle.$$

This step accounts for all the quantum computation that is accomplished in a classically parallel fashion across all nodes of the array.

STEP 2: Measure ("read") all the occupancy probabilities using the following matrix element

$$\begin{aligned} f_1'(x,t) &= \langle\psi'(x,t)|\hat{n}_1|\psi'(x,t)\rangle \\ f_2'(x,t) &= \langle\psi'(x,t)|\hat{n}_2|\psi'(x,t)\rangle \end{aligned}$$

on all sites. In practice, f_1 and f_2 must be determined by either repeated measurement of a single realization of the system or by a single measurement over a statistical ensemble of systems.

STEP 3: Reinitialize ("write") the state of the quantum computer as a separable state where each qubit is set as follows

$$\begin{aligned} |q_1(x,t+\tau)\rangle &= \sqrt{f_1'(x-\ell,t)}|1\rangle + \sqrt{1-f_1'(x-\ell,t)}|0\rangle \\ |q_2(x,t+\tau)\rangle &= \sqrt{f_2'(x+\ell,t)}|1\rangle + \sqrt{1-f_2'(x+\ell,t)}|0\rangle \end{aligned}$$

for all x. Note that qubit $|q_1\rangle$ is shifted to its neighboring node at the left and $|q_2\rangle$ is shifted to its neighboring node at the right. This step requires nearest-neighbor classical communication between all lattice nodes.

ONE TIME-STEP UPDATE COMPLETED.

4 Model Analysis

To model the diffusion equation, we use the following symmetric collision operator

$$\hat{U} = \begin{pmatrix} 1 & 0 & 0 & 0 \\ 0 & \frac{1}{2}-\frac{i}{2} & \frac{1}{2}+\frac{i}{2} & 0 \\ 0 & \frac{1}{2}+\frac{i}{2} & \frac{1}{2}-\frac{i}{2} & 0 \\ 0 & 0 & 0 & 1 \end{pmatrix}, \tag{10}$$

which is obtained from Equation (8) by choosing the "Euler" angles $\phi = -\frac{\pi}{4}$, $\theta = \frac{\pi}{4}$, $\xi = 0$, and $\zeta = \frac{\pi}{2}$. We have inserted the phase factor $e^{-i\frac{\pi}{4}}$ which does not affect the outcome of the collision process, but which is nevertheless needed for a rigorous and strict definition of *local equilibrium* defined below in Equation (19). With this collision operator, the outgoing occupancy probabilities f_1' and f_2' are computed from the incoming occupancy probabilities f_1 and f_2 according to step 2 of the algorithm specified in the previous section

$$\begin{aligned} f_1' &= \langle\psi|\hat{U}^\dagger\hat{n}_1\hat{U}|\psi\rangle \\ f_2' &= \langle\psi|\hat{U}^\dagger\hat{n}_2\hat{U}|\psi\rangle, \end{aligned} \tag{11}$$

where $|\psi\rangle = (\sqrt{f_1}|1\rangle + \sqrt{1-f_1}|0\rangle) \otimes (\sqrt{f_2}|1\rangle + \sqrt{1-f_2}|0\rangle)$, as stated in §3. These functional relations between the outgoing and incoming probabilities reduce to

the following equations

$$f_1' = f_1 f_2 + \frac{1}{2}\left|\sqrt{f_1(1-f_2)} + i\sqrt{(1-f_1)f_2}\right|^2 = \frac{1}{2}(f_1+f_2) \qquad (12)$$
$$f_2' = f_1 f_2 + \frac{1}{2}\left|i\sqrt{f_1(1-f_2)} + \sqrt{(1-f_1)f_2}\right|^2 = \frac{1}{2}(f_1+f_2).$$

According to this prescription, Equation (12) is guaranteed to keep the mass at a site conserved

$$f_1' + f_2' = f_1 + f_2. \qquad (13)$$

We can express the collision Equation (11) along with the streaming operation as a single lattice Boltzmann equation

$$f_a(x + e_a\ell, t+\tau) = f_a(x,t) + \Omega_a, \qquad (14)$$

where the collision term Ω_a is expressible in standard factorizable form. In a classical lattice-gas system, usually the collison term can be written in factorized form at the mesoscopic scale if particle-particle correlations can be neglected. That is, if the assumption of molecular chaos is a good one, than the collision term in general is factorizable so that the probability of occurrence of a local collision configuration is the product of the probability of the occupancy of the local states within that configuration. In a quantum lattice-gas system, the collision term is also factorizable so long as measurements are performed, on a site-by-site basis, which destroys the quantum correlations between particles.

$$\Omega_a \equiv \langle\psi|\hat{U}^\dagger \hat{n}_a \hat{U} - \hat{n}_a|\psi\rangle = \frac{1}{2}\left[f_{a+1}(1-f_a) - f_a(1-f_{a+1})\right], \qquad (15)$$

for $a = 1, 2$ and where $e_1 = 1$ and $e_2 = -1$. The lattice Boltzmann equation Equation (14) can be linearized by expanding the collision term to first order in the fluctuation [11, 12], $\Omega_a \simeq \sum_b J_{ab}\delta f_b$, where the Jacobian matrix is

$$J = \begin{pmatrix} \frac{\partial\Omega_1}{\partial f_1} & \frac{\partial\Omega_1}{\partial f_2} \\ \frac{\partial\Omega_2}{\partial f_1} & \frac{\partial\Omega_2}{\partial f_2} \end{pmatrix} = \frac{1}{2}\begin{pmatrix} -1 & 1 \\ 1 & -1 \end{pmatrix}. \qquad (16)$$

The eigenvalues and eigenvectors of J characterize the behavior of a lattice-gas system in the long-wavelength and low frequency limit. The eigenvalues of J are $\lambda_1 = 0$ and $\lambda_2 = -1$, with eigenvectors $\vec{\xi}_1 = (1,1)$ and $\vec{\xi}_2 = (-1,1)$, respectively. The conserved macroscopic field corresponding to the zero eigenvalue is the mass-density field

$$\rho = \vec{\xi}_1 \cdot (f_1, f_2) = f_1 + f_2 \qquad (17)$$

as expected.

Local equilibrium of the mass-density field, $\rho^{\text{eq}} \equiv d$, occurs when the on-site particle distribution causes the collision term to vanish, $\Omega_a|_{f=f^{\text{eq}}} = 0$, for all a. In the present case, this occurs when the occupancy probability of the left and right channels are equal

$$f_1^{\text{eq}} = f_2^{\text{eq}} = \frac{d}{2}, \qquad (18)$$

which is evident from Equation (15). Local equilibrium of the system can also be defined in terms of the collision operator $\hat{U}$ by the following constraint

$$\hat{U}|\psi^{\rm eq}\rangle = |\psi^{\rm eq}\rangle, \tag{19}$$

which is also evident from Equation (15) since in this situation $\Omega_a|_{\psi=\psi^{\rm eq}} = 0$. Now if we explicitly write out Equation (19) in matrix form

$$\begin{pmatrix} 1 & 0 & 0 & 0 \\ 0 & \frac{1}{2}-\frac{i}{2} & \frac{1}{2}+\frac{i}{2} & 0 \\ 0 & \frac{1}{2}+\frac{i}{2} & \frac{1}{2}-\frac{i}{2} & 0 \\ 0 & 0 & 0 & 1 \end{pmatrix} \begin{pmatrix} \sqrt{f_1^{\rm eq}}\sqrt{f_2^{\rm eq}} \\ \sqrt{f_1^{\rm eq}}\sqrt{1-f_2^{\rm eq}} \\ \sqrt{1-f_1^{\rm eq}}\sqrt{f_2^{\rm eq}} \\ \sqrt{1-f_1^{\rm eq}}\sqrt{1-f_2^{\rm eq}} \end{pmatrix} = \begin{pmatrix} \sqrt{f_1^{\rm eq}}\sqrt{f_2^{\rm eq}} \\ \sqrt{f_1^{\rm eq}}\sqrt{1-f_2^{\rm eq}} \\ \sqrt{1-f_1^{\rm eq}}\sqrt{f_2^{\rm eq}} \\ \sqrt{1-f_1^{\rm eq}}\sqrt{1-f_2^{\rm eq}} \end{pmatrix} \tag{20}$$

we see that the following two equations must be satisfied

$$\begin{aligned} \frac{e^{-i\frac{\pi}{4}}}{\sqrt{2}}\left(\sqrt{f_1^{\rm eq}}\sqrt{1-f_2^{\rm eq}} + i\sqrt{1-f_1^{\rm eq}}\sqrt{f_2^{\rm eq}}\right) &= \sqrt{f_1^{\rm eq}}\sqrt{1-f_2^{\rm eq}} \qquad (21) \\ \frac{e^{-i\frac{\pi}{4}}}{\sqrt{2}}\left(i\sqrt{f_1^{\rm eq}}\sqrt{1-f_2^{\rm eq}} + \sqrt{1-f_1^{\rm eq}}\sqrt{f_2^{\rm eq}}\right) &= \sqrt{1-f_1^{\rm eq}}\sqrt{f_2^{\rm eq}}. \end{aligned}$$

If $f_1^{\rm eq} = f_2^{\rm eq} \equiv \frac{d}{2}$, these local equilibrium conditions reduce to the single identity

$$\frac{e^{-i\frac{\pi}{4}}}{\sqrt{2}}(1+i) = 1. \tag{22}$$

Therefore, we now see why it is necessary to include the phase factor $e^{-i\frac{\pi}{4}}$ in the definition of the collision operator so that $\hat{U}$ has an eigenvalue of unity value with an eigenvector corresponding to a local equilibrium configuration.

To derive an effective field theory at the macroscopic scale, let us suppose the lattice-gas system is everywhere in local equilibrium. That is, let us suppose that after the collision step $f_1(x) = f_2(x) = \frac{d(x)}{2}$ at all sites of the lattice. Then, without loss of generality, let us consider the particle distributions centered about x before and after application of the streaming operator. Letting the top row denote the f_1 occupancy probabilities and the bottom row the f_2 occupancy probabilities, if before streaming we have

$$\begin{array}{ccccccc} \ldots & \frac{d(x-2\ell)}{2} & \frac{d(x-\ell)}{2} & \frac{d(x)}{2} & \frac{d(x+\ell)}{2} & \frac{d(x+2\ell)}{2} & \ldots \\ \ldots & \frac{d(x-2\ell)}{2} & \frac{d(x-\ell)}{2} & \frac{d(x)}{2} & \frac{d(x+\ell)}{2} & \frac{d(x+2\ell)}{2} & \ldots, \end{array}$$

then after streaming the occupancy probabilities would be shifted as follows

$$\begin{array}{ccccccc} \ldots & \frac{d(x-\ell)}{2} & \frac{d(x)}{2} & \frac{d(x+\ell)}{2} & \frac{d(x+2\ell)}{2} & \frac{d(x+3\ell)}{2} & \ldots \\ \ldots & \frac{d(x-3\ell)}{2} & \frac{d(x-2\ell)}{2} & \frac{d(x-\ell)}{2} & \frac{d(x)}{2} & \frac{d(x+\ell)}{2} & \ldots. \end{array}$$

The density, $\rho(x,t) = f_1(x,t) + f_2(x,t)$, at site x before streaming is $\rho(x,t) = d(x)$ and the density at site x after streaming is $\rho(x,t+\tau) = \frac{1}{2}[d(x+\ell) +$

$d(x-\ell)]$. Therefore, the first finite-difference in time of the mass-density field is expressible as a second-order difference in space

$$\rho(x,t+\tau)-\rho(x,t)=\frac{1}{2}[d(x+\ell)-2d(x)+d(x-\ell)] \tag{23}$$

or

$$\rho(x,t+\tau)-\rho(x,t)=\frac{1}{2}[\rho(x+\ell,t)-2\rho(x,t)+\rho(x-\ell,t)]. \tag{24}$$

In the continuum limit (a fixed box size with the number of lattice points approaching infinity), the mass-density field is continuous and differentiable. Therefore, Taylor expanding about x and t to second order in the Knudsen number[4], Equation (24) can be written in differential point form

$$\frac{\partial\rho(x,t)}{\partial t}=\frac{\ell^2}{2\tau}\frac{\partial^2\rho(x,t)}{\partial x^2}. \tag{25}$$

This is the diffusion equation with a constant transport coefficient of $\frac{\ell^2}{2\tau}$.

5 Numerical Simulation Results

In this section we show several results from one-dimensional numerical simulations of the factorized quantum lattice gas. All the numerical simulations were carried out using Mathematica.

5.1 Delta Function Initial Condition

The algorithm described in §3 for the factorized quantum lattice gas, with two qubits per site, for the diffusion equation has the property that it simulates two non-interpenetrating lattice-gas systems simultaneously. That is, there are two independent "checker-board" sub-lattices. For illustration purposes, let all even numbered cells of the lattice be color-coded white and all the odd numbered cells of the lattice be color-coded black. This defines the two "checker-board" partitions of the lattice. Any particles initially on the black partition collide and stream to the white partition and vice versa. This is because each of the qubits per site move to their nearest neighboring sites which are on the alternate partition. After a second application of the local update rule, the particles return to the original partition. For this reason, particles on the white sub-lattice never interact with those on the black one. This dual-lattice behavior is shown on the left column of Figure 2 which are snapshots of the time evolution at every other time step for a small lattice of size $L=32\ell$. Initially all the particles are located at the center cell of the lattice. There is a delta function peak in the mass-density field

$$\rho(x,0)=\delta(x-\frac{L}{2}), \tag{26}$$

[4] The dimensionless Knudsen number (Kn) is the ratio of the characteristic mean-free-path length to the characteristic macroscopic scale of the entire system. In the present case, Kn is the ratio of the lattice cell size to the size of the box, Kn $\sim \frac{\ell}{L}$.

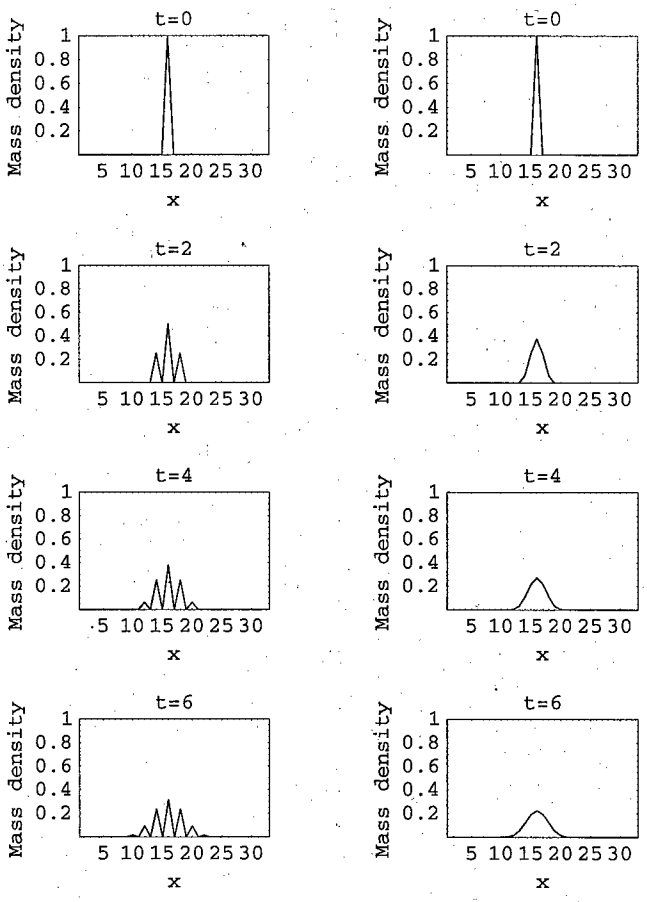

Figure 2: The initial condition of the mass-density field is set to a delta function in the middle of a lattice of size $L = 32\ell$. Snapshots of the time evolution of the mass-density field is shown for the case where both qubits are streamed (left column plots) as described in §3 and also for the case where a single qubits is streamed alternatively in both directions (right column plots) as described in Appendix A. A double lattice effect is observed in the first case and does not occur in the second case with the improved version of the algorithm.

where $\delta(x) = 1$ for $x = 0$ and $\delta(x) = 0$ otherwise. After two time-steps, particles diffuse two lattice cells away from the center point and there are no particles occupying the lattice cells immediately neighboring the center one. The double lattice effect is seen in the subsequent snapshots of the mass-density field.

It is possible to repair this deficiency in the algorithm by allowing only the state of one of the qubits of a cell to be transferred to the neighboring cell. The state of the other qubit in the cell remains fixed. The improved version of the algorithm is described in a step-by-step fashion in Appendix A. With the improved version of the algorithm, the resulting mass-density field is smoothly varying across the lattice cell even in this case with the most discrete initial condition. This is depicted on the right column of Figure 2.

5.2 Broadening of a Gaussian Packet

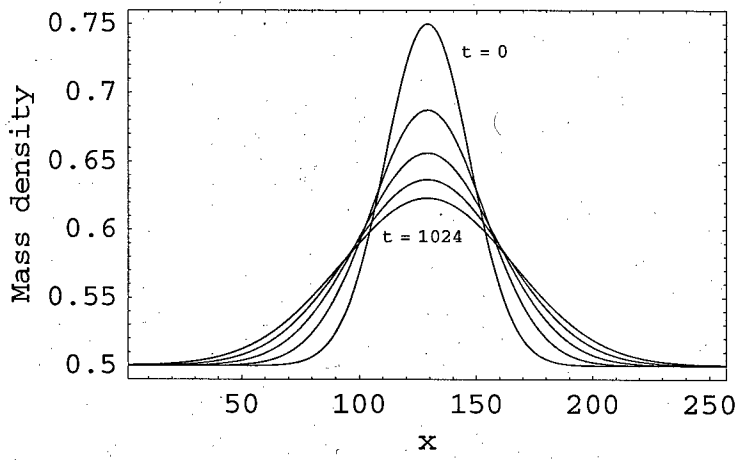

Figure 3: The time evolution of a Gaussian packet of a lattice of size $L = 256\ell$ for $t = 0, 256, 512, 768, 1024\tau$. The packet width is initially $\sigma = 0.1\ell$ and broadens over time as soon in the figure by over plotting.

The next numerical test of the factorized quantum lattice gas demonstrates that the dynamical evolution of its mass-density field is indeed governed by the diffusion equation. The mass-density field is initialized with a Gaussian waveform

$$\rho(x,0) = \frac{1}{4} e^{\frac{(x-\frac{L}{2})^2}{\sigma_\circ^2}} + \frac{1}{2}, \tag{27}$$

where the initial packet width is $\sigma_\circ = \frac{L}{10}\ell$. The Gaussian packet will undergo diffusive broadening as its width, $\sigma(t) = \sqrt{\sigma_\circ^2 + 4Dt}$, increases over time while its peak amplitude decreases at a rate of $\frac{1}{\sigma(t)}$. The exact analytical solution for

the mass-density field at some later time, t, is given by the following expression

$$\rho^{\text{exact}}(x,t) = \frac{1}{4}\frac{\sigma_\circ}{\sqrt{\sigma_\circ^2 + 4Dt}} e^{\frac{(x-\frac{L}{2})^2}{\sigma_\circ^2+4Dt}} + \frac{1}{2}, \tag{28}$$

where the diffusion constant is $D = \frac{1}{2}\frac{\ell^2}{\tau}$.

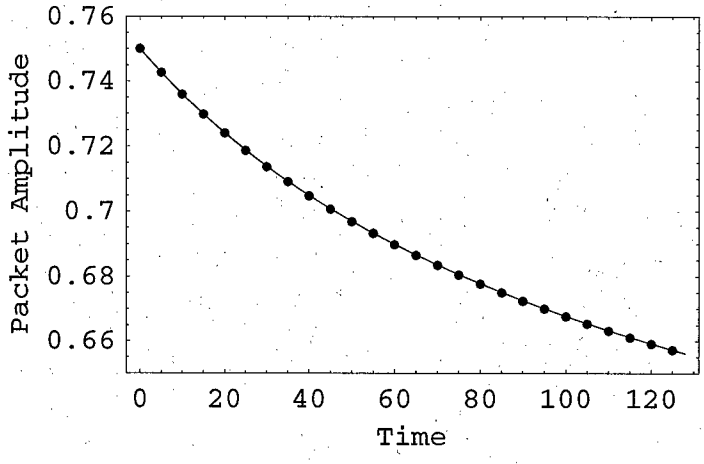

Figure 4: Time series plot of the temporal decay of a Gaussian packet of a lattice of size $L = 128\ell$ for $t = 0$ up to $t = 128\tau$. The packet width is initially $\sigma = \frac{L}{10}\ell$ and broadens in time as $\sigma = \sqrt{\sigma_\circ + 4Dt}$ where the initial width is $\sigma_\circ = 0.1\ell$ and the diffusion constant is $D = \frac{1}{2}\frac{\ell^2}{\tau}$. The packet's amplitude decays at a rate of $\frac{1}{\sigma}$, which is the exact solution plotted as the solid curve. The plotted data (black circles) taken from the numerical simulation of the factorized quantum lattice gas are in excellent agreement with the exact analytical solution.

The dispersion rate of the packet can be directly determined by measuring the decay rate of the peak, since the peak amplitude is proportional to the inverse of the packet width. The numerical data extracted from the simulation is plotted along with the exact analytical solution in Figure 4. The agreement between the numerical simulation and the exact analytical solution is excellent, which confirms that the dynamical space-time evolution of the mass-density field is governed by the parabolic diffusion equation.

5.3 Exponential Decay of a Sinusoidal Perturbation

As another test of the factorized quantum lattice-gas model, let us consider an example problem to illustrate diffusive damping in the continuum limit. We begin with a lattice with $L = 128\ell$ sites (or nodes). The mass density field is initially set to be a sine wave

$$\rho(x,0) = \frac{1}{4}\sin\frac{2\pi x}{L} + \frac{1}{2}. \tag{29}$$

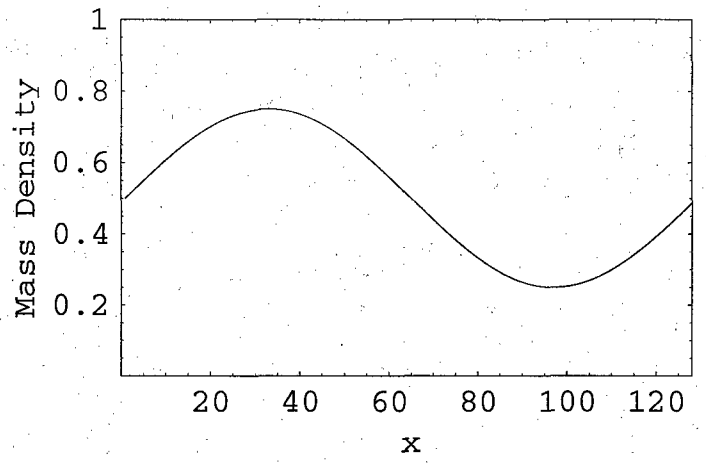

Figure 5: Initial sinusoidal perturbation in the mass-density field about a background density at half-filling $d_\circ = \frac{1}{2}$ for a lattice of size $L = 128\ell$.

This initial mass-density profile is plotted in Figure 5. The boundary conditions are periodic and remain fixed at all time

$$\rho(0,t) = \rho(L,t) = \frac{1}{2}. \tag{30}$$

After repeated application of the collision and streaming operators of the factorized quantum lattice gas, the amplitude of the mass-density wave is observed to decay in time. To be a solution of the diffusion equation Equation (25), the mass-density field must have the form

$$\rho^{\text{exact}}(x,t) = \frac{1}{4} e^{-\Gamma t} \sin \frac{2\pi x}{L} + \frac{1}{2}, \tag{31}$$

where the damping constant is $\Gamma = Dk^2$, the wave number is $k = \frac{2\pi}{L}$, and the diffusion constant is $D = \frac{1}{2}\frac{\ell^2}{\tau}$. This is in fact observed in the numerical simulation which indicates exponential decay of the mass-density profile, as shown in Figure 6.

A final test of the factorized quantum lattice-gas algorithm as a model of the diffusion equation is the measurement of its numerical convergence. Multiple simulations (10 in total) were carried out for lattice sizes ranging from $L = 64\ell, 128\ell, 256\ell, \ldots$ up to $L = 32768\ell$. In each case the initial state of the simulation was a sinusoidal perturbation of the mass-density field about half-filling according to Equation (29). Each simulation was run for $T = 64\tau$ time-step iterations and the numerical error, denoted ϵ, from the exact solution

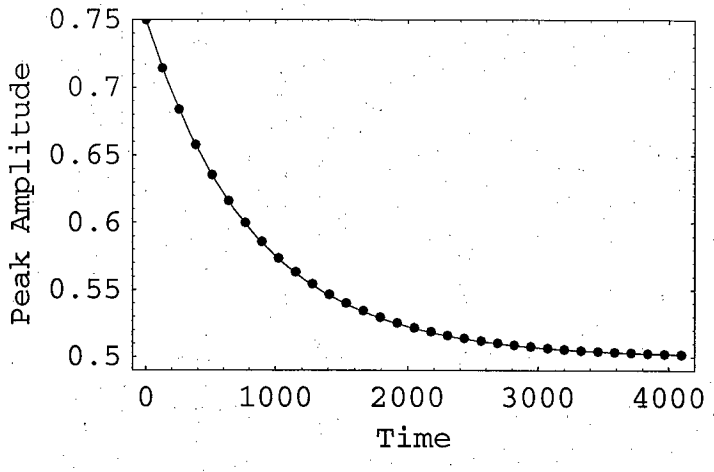

Figure 6: Exponential damping of a sinusoidal profile by action of mass diffusion. The solid curve is the predicted envelope $\frac{1}{4}e^{-\frac{1}{2}(\frac{2\pi}{128})^2} + \frac{1}{2}$. The plotted data (black circles) taken from the numerical simulation of the factorized quantum lattice gas are in excellent agreement with the theoretical envelope.

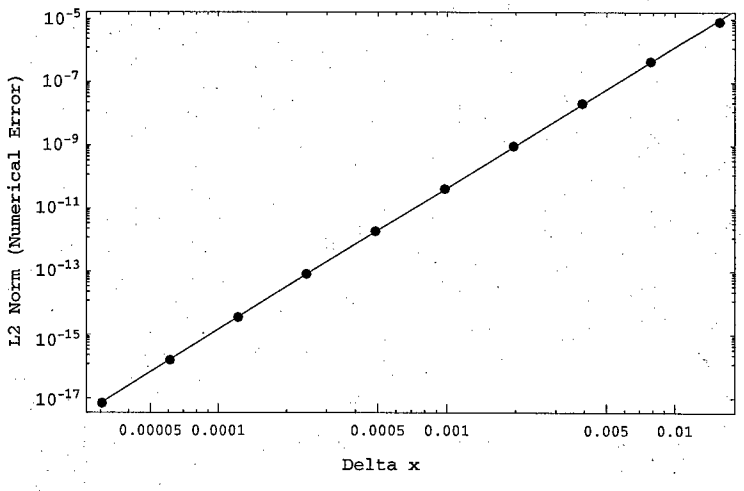

Figure 7: Log-log plot of the numerical error versus resolving grid cell size, δx, indicating the the convergence property of the factorized quantum lattice-gas algorithm for the diffusion equation described in §3. The data (black circle) are taken from numerical simulations with grid sizes from $L = 64\ell$ up to 32768ℓ with a fixed number of time steps $T = 64\tau$. The solid curve is a best-fit linear regression with a slope of 4.471 indicating at least second-order convergence in space.

was then measured using the following formula

$$\epsilon(L) = \frac{1}{L}\sqrt{\sum_{x=1}^{L}\left[\rho(x) - \rho^{\text{exact}}(x)\right]^2}, \tag{32}$$

where the exact solution for the mass-density field is

$$\rho^{\text{exact}}(x) = \frac{1}{4}e^{-\frac{1}{2}(\frac{2\pi}{L})^2 T}\sin\frac{2\pi x}{L} + \frac{1}{2}. \tag{33}$$

We define the grid resolution as the inverse of the total number of lattice points. That is, for a box of size 1, the *resolving cell size* is defined as $\delta x \equiv \frac{1}{L}$. A plot of the error versus the resolution is given in Figure 7. As the resolution is increased, the error drops off as $\epsilon(L) \sim L^{4.471}$. The factorized quantum lattice-gas algorithm has numerical convergence that is at least second-order accurate in space and first-order accurate in time.

6 Conclusion

In this paper, we illustrated a factorized quantum lattice-gas algorithm that can be used to model the behavior of a mass-density field governed by the diffusion equation. For simplicity, the model is worked out in one-dimension, but can straightforwardly be generalized to higher dimensions.[5] All the algorithmic steps needed to implement the model were explicitly laid out. Furthermore, to validate the model, several numerical tests were performed in Mathematica simulations to check the numerical stability of the algorithm and to check whether the dynamical behavior of the quantum lattice-gas system behaves as expected.

To test numerical stability, an initial mass-density profile with maximally steep gradients was used: a delta function. No numerical overflow occurred and the algorithm remained unconditionally stable regardless of the number of time steps. It was noted that two independent sub-lattices are simultaneously simulated in the simplest form of the quantum algorithm, but this can be remedied using an improved version of the algorithm given in the appendix. Symmetrical broadening of a Gaussian packet was also tested and the macroscopic behavior of the model matched the analytical solution of dispersion in the diffusion equation. Finally, the decay of a sinusoidal profile was tested and the comparison of the numerical to the analytical result was also presented in this paper. The amplitude of the sinusoidal profile decays exponentially in time while the profile remains a perfect sinusoid, and agrees with the analytical solution for damping in the diffusion equation. These numerical tests conclusively demonstrate that the macroscopic dynamics of this factorized quantum lattice-gas model is indeed governed by a parabolic diffusion equation. The factorized quantum lattice-gas

[5] In a 2D or 3D simulation, for example, still only two qubits per site is required as in the 1D case. This is because the 1D update rules, Equation (14), can be applied along each dimension independently in succession.

algorithm was found to numerically convergence to the exact analytical solutions with first-order accuracy in time and second-order accuracy in space.

The reason for using this quantum lattice-gas algorithm over say an unconditionally stable classical implicit algorithm known for diffusion is that this quantum algorithm can be directly implemented on a type-II quantum computer whereas known classical algorithms cannot because of their non-unitary formulations. For the quantum lattice-gas algorithm to be implemented on a quantum computer with an array of qubits that can only be superposed and entangled for a short duration and only over short distances, periodic ensemble measurement of all the occupancy probabilities must occur at each and every time step. The measurement process breaks the unitarity of the algorithm, but does so in the least destructive of ways. The measurement process gives rise to a kind of controlled decoherence that mimics the effect of molecular chaos in classical many-body kinetic theory. Therefore, the measurement process causes the collision term in the quantum lattice-Boltzmann equation to be expressible in a factorized or "mean-field" form. The subsequent collapse of the wavefunction into a tensor product state is done in such way as to conserve the local mass at each site, and thereby conserves the total mass of the system. Furthermore, given the measurement process, the mesoscopic lattice-gas dynamics is described by a lattice-Boltzmann equation that obeys the principle of detailed balance.

All quantum lattice-gas algorithms are unconditionally stable during the course of the simulation run, including this algorithm for the diffusion equation, when implemented on a conventional classical computers where the round off error of the floating-point representation (using say a 64-bit word with a 52-bit mantissa) of real valued quantities is on the order of a part in 10^{15}. The stability of the quantum lattice-gas algorithm derives from the representation of the collision operator by a unitary matrix. Yet the stability of the algorithm running on a type-II quantum computer will depend on the accuracy limitations for measuring the expectation values of the binary states, representing the desired quantum gate by control pulses, and re-preparing the quantum wavefunction during every time step iteration.

This last point can be analytically derived in the most general situation where the unitary collision matrix, Equation (8), has an arbitrary set of Euler angles. In the case when $\zeta = \xi$, the diffusion equation becomes the governing effective macroscopic field equation. However, in the more general case when $\zeta \neq \xi$, the governing field equation is the nonlinear Burger's equation. The analysis and numerical simulation of the factorized quantum lattice gas in this general case is treated in a subsequent paper [13].

It is not claimed here that the computational complexity of simulating the one-dimensional diffusion equation is reduced in any way by exploiting efficient parallel computation derived from using the quantum mechanical principle of superposition of states. In fact, in the present model, only the quantum states of two qubits are in superposition any time following a quantum gate operation and prior to measuring the expectation value of the binary states of each qubit. The quantum gate operation is represented by a 4×4 unitary matrix. Therefore, from

a classical point-of-view, its action is computationally equivalent to multiplying a 4-component complex vector by a 16 component unitary matrix. This in turn is equivalent to 64 floating-point multiplies and 640 floating-point additions, or 704 floating-point operations in total. A present day classical computer running at a gigaflop rate could compute this quantum gate operation in under a microsecond. In contrast, in the NMR-based type-II quantum computer using the chloroform molecule for example, the gate operation occurs within one spin-spin decoherence time, and one step of the algorithm isn't repeated until after the spin relaxation time, about half a minute for chloroform. Therefore, there is no speed-up obtained in the quantum apparatus versus a conventional gigaflop desktop computer. However, if a more complex quantum lattice-gas model were implemented with n qubits per node where n is a large number, the classical computer would have to do a matrix multiply of size $2^n \times 2^n$, so the total number of required floating-point operations scales exponentially in n. Therefore, a type-II quantum computer implementation of a quantum lattice-gas algorithm could outperform any classical computer implementation of the same algorithm when the number of qubits per node is large, provided the number of control pulses needed to implement the $2^n \times 2^n$ unitary matrix as a sequence of quantum gate operations scales polynomially in n. We are currently trying to experimentally determine the scaling behavior of the number of required control pulses versus the number of qubits per node and this will be presented in a subsequent paper. The quantum algorithm for the one-dimensional diffusion equation serves as a test case in this regard.

7 Acknowledgements

I would like to thank J.M. Powers for his suggestion to me to apply the quantum lattice-gas method to the problem of modeling the one-dimensional diffusion equation so that it might be compared, on strictly classical numerical modeling grounds, with conventional numerical techniques. His comments on the draft version of this manuscript were greatly appreciated. I would also like to thank B.M. Boghosian for many helpful discussions regarding this quantum lattice-gas model. Finally, I would like to acknowledge D. Cory and M. Pravia for their help in designing and testing an NMR-based type-II quantum computer prototype capable of running the quantum algorithm presented here.

References

[1] Jeffrey Yepez. Type-ii quantum computers. *International Journal of Modern Physics C*, 12(9):1–12, 2001. Presented at the Quantum Computing Colloquium, MIT Nuclear Engineering Department, September 27, 1999 and at the Air Force Office of Scientific Research Computational and Applied Mathematics Meeting 2000, Stanford University, June 28, 2000.

[2] Bruce M. Boghosian and C. David Levermore. A cellular automaton for burger's equation. *Complex Systems*, 1:17–29, 1987.

[3] Y. H. Qian, D. d'Humières, and P. Lallemand. Diffusion simulation with a deterministic one-dimensional lattice-gas model. *Journal of Statistical Physics*, 68(3/4):563–573, 1992.

[4] Richard P. Feynman. Quantum mechanical computers. *Optics News*, 11(2):11–20, 1985.

[5] David Deutsch. Quantum computational networks. *Proceedings of the Royal Society, London*, A(425):73–90, 1989.

[6] David P. DeVincenzo. Two-bit gates are universal for quantum computation. *Physical Review A*, 51:1015–1022, 1995.

[7] Adriano Barenco, Charles H. Bennett, Richard Cleve, David P. DeVincenzo, Norman H. Margolus, Peter W. Shor, Tycho Sleator, John Smolin, and Harald Weinfurter. Elementary gates for quantum computation. *Physical Review A*, 52(5):3457–3467, 1995.

[8] Adriano Barenco. A universal two-bit gate for quantum computation. *Proceedings Royal Society London*, 449A:679–683, 1995.

[9] Jeffrey Yepez. Lattice-gas quantum computation. *International Journal of Modern Physics C*, 9(8):1587–1596, 1998. Proceeding of the 7th International Conference on the Discrete Simulation of Fluids, University of Oxford.

[10] Jeffrey Yepez. Quantum computation of fluid dynamics. In Collin P. Williams, editor, *Quantum Computing and Quantum Communications*, page 480pp. Lecture Notes in Computer Science, Springer-Verlag, 1999. First NASA International Conference, QCQC'98, Palm Springs, California, USA, February 17-20, 1998, Selected Papers.

[11] S.P. Das, H.J. Bussemaker, and M.H. Ernst. Generalized hydrodynamics and dispersion relations in lattice gases. *Physical Review E*, 48(1):245–255, 1993.

[12] H.J. Bussemaker, M.H. Ernst, and J.W. Duffy. Generalized boltzmann equation for lattice gas automata. *Journal of Statistical Physics*, 78(5/6):1521–1554, 1995.

[13] Jeffrey Yepez. Quantum lattice-gas model for burger's equation. *Journal of Statistical Physics*, To appear 2001. Presented at the 9th International Conference on Discrete Simulation of Fluid Dynamics, Santa Fe, NM, August 22, 2000.

A Improved Algorithm

The algorithm described in this appendix uses a variant of the typical lattice-gas update procedure. First of all, there are two particles per site, but only one of them is a moving particle. The other is a stationary or rest particle. The moving particle hops in both directions (and this is not typical in lattice-gas models). The collision operator is homogeneously applied across the lattice and then the moving particle hops one lattice unit to the right. The collision operator is then homogeneously applied again across the entire lattice and then the moving particle hops one lattice unit to the left. The moving particle must hop in both directions to keep the macroscopic dynamics unbiased and symmetrical. Therefore, each and every time step involves two applications of the collision operator and streaming operator.

The factorized quantum lattice-gas algorithm for the one-dimensional diffusion equation can be implemented with two passes as defined in the following six steps (two groups of three). This version of the algorithm is considered to be an improvement over the simpler version given in §3 because it remedies the problems of coexisting independent sub-lattices. Spurious high frequency noise is thereby removed from the time variation of the macroscopic mass-density field as well. We assume the initial state of the quantum computer is set as specified in Figure 1, where $|q_a(x,t)\rangle = \sqrt{f_a(x,t)}|1\rangle + \sqrt{1-f_a(x,t)}|0\rangle$.

STEP 1: Apply the collision operator simultaneously to all sites

$$|\psi'(x,t)\rangle = \hat{U}|\psi(x,t)\rangle.$$

This step accounts for all the quantum computation that is accomplished in a classically parallel fashion across all nodes of the array.

STEP 2: Measure ("read") all the occupancy probabilities using the following matrix elements

$$\begin{aligned} f_1'(x,t) &= \langle\psi'(x,t)|\hat{n}_1|\psi'(x,t)\rangle \\ f_2'(x,t) &= \langle\psi'(x,t)|\hat{n}_2|\psi'(x,t)\rangle \end{aligned}$$

on all sites. In practice, f_1 and f_2 must be determined by either repeated measurement of a single realization of the system or by a single measurement over a statistical ensemble of systems.

STEP 3: Reinitialize ("write") the state of the quantum computer as a separable state where each qubit is set as follows

$$\begin{aligned} |q_1(x,t+\tau)\rangle &= \sqrt{f_1'(x,t)}|1\rangle + \sqrt{1-f_1'(x,t)}|0\rangle \\ |q_2(x,t+\tau)\rangle &= \sqrt{f_2'(x+\ell,t)}|1\rangle + \sqrt{1-f_2'(x+\ell,t)}|0\rangle \end{aligned}$$

for all x. Note that qubit $|q_2\rangle$ is shifted to its neighboring node at the right. This step requires nearest-neighbor classical communication between all lattice

nodes.

STEP 4: Apply the collision operator again as in STEP 1.

STEP 5: Measure ("read") the occupancy probabilities again as in STEP 2.

STEP 6: Reinitialize ("write") the state of the quantum computer as a separable state where each qubit is set as follows

$$|q_1(x,t)\rangle = \sqrt{f_1(x,t)}|1\rangle + \sqrt{1-f_1(x,t)}|0\rangle \quad (34)$$

$$|q_2(x,t)\rangle = \sqrt{f_2(x-\ell,t)}|1\rangle + \sqrt{1-f_2(x-\ell,t)}|0\rangle \quad (35)$$

for all x. Note that qubit $|q_2\rangle$ is shifted to its neighboring node at the left. This step requires classical communication between all lattice nodes.

ONE TIME-STEP UPDATE COMPLETED.

With this improved version of the quantum algorithm, the diffusion constant that arises in the effective field theory is $D^{\text{imp}} = \frac{1}{4}\frac{\ell^2}{\tau}$, half the value the diffusion constant that arises from the simpler version of the algorithm presented in §3. The reason for the reduction in dissipation is that the diffusion constant goes as the ratio of the square of the mean-free path length to the mean-free collision time. In the simple version of the quantum algorithm, the mean-free path length goes as the lattice cell size ℓ and the mean-free collision time is the time of a single update τ. However, in the improved version of the algorithm, the collision frequency is doubled, so effectively both the mean-free path length and the mean-free collision time are halved. Consequently, the value of the transport coefficient is halved, $D^{\text{imp}} = \frac{D}{2}$.